Back-stepping Active Disturbance Rejection Control for Attitude Control of Aircraft Systems Based on Extended State Observer

Huixuan Zhuang, Q. L. Sun, Z. Q. Chen, Xianyi Zeng

International Journal of Control, Automation and Systems 19(6) (2021) 2134-2149
http://dx.doi.org/10.1007/s12555-019-1029-x
ISSN:1598-6446 eISSN:2005-4092
http://www.springer.com/12555

Back-stepping Active Disturbance Rejection Control for Attitude Control of Aircraft Systems Based on Extended State Observer

Huixuan Zhuang*, Qinglin Sun*, Zengqiang Chen, and Xianyi Zeng

Abstract: Robust flight control laws based on back-stepping technology and ADRC method are designed for attitude control of a non-linear aircraft system. First, non-linear aircraft model is introduced and converted to standard equation of state. Then, the extended state observer is applied to estimate the unknown variables, the homologous ADRC is designed to ensure the state variables of the CLS to astringe to the reference state. Next, the stability of ESO and ADRC are analyzed and proven theoretically. At last, the effectiveness of this method is illustrated by extensive comparative simulations. The results acquired from simulation attest that ADRC can achieve better control performance than PID and SMC method.

Keywords: Active disturbance rejection control, aircraft attitude control, back-stepping technique, extended state observer.

NOMENCLATURE

Abbreviation

ADRC	Active disturbance rejection control
CLS	Closed-loop system
AFCS	Automatic flight control system
UUB	Uniformly ultimately bounded
ESO	Extended state observer
PID	Proportion Integration Differentiation
SMC	Sliding mode control
TD	Tracking differentiator

Variables

S_g	Ground coordinate system
S_h	Local horizontal system
S_w	Wind coordinate frame
S_s	Stability axes system
S_a	Airframe coordinate system
S_b	Body axes system
χ	Heading angle
γ	Flight path angle
μ	Velocity roll angle
ψ	Yaw angle
θ	Pitch angle
ϕ	Roll angle
α	Angle of attack
β	Sideslip angle
D, L, Q	Drag, lift, and side forces, respectively
g	Gravitational acceleration
T_x	Thrust
p, q, r	Angular velocity components
$\delta_a, \delta_r, \delta_e$	Deflection angle vector of aileron, elevator, rudder
$\Delta\alpha, \Delta V$	Perturbations from the trim values
V_0	Trim velocity
V	Velocity of aircraft
C_l, C_m, C_n	Moment coefficients of roll, pitch and yaw, respectively
S_r	Reference area
$\mathcal{L}$	Reference lateral or longitudinal lengths
I_x, I_y, I_z	Principal moments of inertia
ρ	Air density
M_a	Mach number

Manuscript received December 10, 2019; revised August 4, 2020; accepted September 22, 2020. Recommended by Associate Editor Aldo Jonathan Munoz-Vazquez under the direction of Editor Chan Gook Park. The work was prepared at the College of Artificial Intelligence, Nankai University and was supported by the National Natural Science Foundation of China (No. 61973172, 61973175) and the Key Technologies R&D Program of Tianjin under Grant 19JCZDJC32800.

Huixuan Zhuang, Qinglin Sun, and Zengqiang Chen are with the College of Artificial Intelligence, Nankai University, Tianjin 300350, China and the Intelligent Robots Key Laboratory, Nankai University, Tianjin 300350, China (e-mails: hxzhuang0123@mail.nankai.edu.cn, {sunql, chenzq}@nankai.edu.cn). Xianyi Zeng is with University of Lille 1, Nord deFrance, 59000 Lille, France and GEMTEX Laboratory, ENSAIT, Roubaix 59100, France (e-mail: xianyi.zeng@ensait.fr).
* Corresponding authors.

m	Aircraft mass
x, y, z	Inertial position coordinates

1. INTRODUCTION

1.1. Research background

The development of modern automatic control system plays a significant role in the progress of modern flight control, especially in the development of civil and military aviation. Since the 1960s, AFCS has been the main application field of control methods [1]. In AFCS, there is not only pitch attitude controller but also roll and yaw controllers. Attitude control system is no exception, and its nonlinear dynamics must also be considered [2]. Various nonlinear control algorithms, such as fault tolerant control [3–5], that studied H_∞ fault tolerant attitude control of satellite with actuator and sensor faults based on observer; fuzzy adaptive algorithm [6,7]; variable structure control [8]; and sliding control [9,10], that studied the fixed time integral sliding mode control for the attitude stability of the quadrotor unmanned aerial vehicle with actuator failure; etc., have been proposed for solving the attitude control problem for spacecraft. However, so far, few scholars have studied the attitude control of aircraft by using ADRC; it is rare to study this problem in combination with the back-stepping method.

In fact, some scholars have applied ADRC or ESO to study aircraft systems, such as, the trajectory linearization control of hypersonic reentry vehicle is studied by using active disturbance rejection [11]; Wang *et al*. studied the trajectory tracking of a vertical takeoff and landing UAV using interference suppression control [12]; Mokhtari *et al*. used disturbance observer and extended observer to study hierarchical control of coaxial rotor UAV [13,14]. However, no one has applied the back-stepping active disturbance rejection control method to study the attitude control of aircraft.

1.2. Research motivation

The application of the optimal control model of human pilot in the attitude control system of aircraft is studied in [15], this paper studies the application of the optimal control model of human pilot in the attitude control system of the aircraft. His emphasis is to study the role of the best control model of the pilot in the attitude control of the aircraft rather than the attitude control of the aircraft. Most of them are related to four rotor aircraft.

The attitude control of an aircraft is to maintain a stable attitude during the flight process, and at the same time, according to the sudden situation of the air environment, the aircraft is required to make an appropriate attitude change. At this time, the requirement of attitude control is particularly important. In recent years, there have been frequent air accidents, and it has to be mentioned that the Sichuan Airlines alternate landing event that attracted global attention in 2018. When the windshield is broken and the aircraft equipment is completely out of order, Captain Liu Chuanjian can only make a successful alternate by himself. During the alternate process, he needs to adjust the flight attitude constantly for many times, the attitude control is very crucial. Thus, we have the idea of studying the attitude control of aircraft.

1.3. Research technology

The basic idea of back-stepping design method is to decompose the complex nonlinear system into subsystems that do not exceed the order of the system, and then design some Lyapunov functions and intermediate virtual control variables for each sub-system, all the way back to the whole system, and integrate them to complete the design of the whole control law. The virtual control law is designed to guarantee some performance of the kernel system, such as stability, etc.; then the algorithm of the virtual control law is modified step by step, but the given performance should be guaranteed; then the real stabilizing controller is designed to realize the global regulation or tracking of the system, so that the system can reach the expected performance index. In recent years, back-stepping has been widely used in flight control systems and aircraft control systems [16–18]. Fu *et al*. [16] applied a method, which is an adaptive neural network back-stepping dynamic surface control algorithm based on asymmetric time-varying *Barrier Lyapunov Function*, for the attitude system of a unmanned aerial vehicle. In [17], a flight table with one degree of freedom was studied by using back-stepping SMC. Zhang *et al*. [18] proposed a method, that is combining the sliding mode disturbance observer and the back-stepping technique, to apply to a flight control system for heavy cargo airdrop operations.

Han [19] originated a unique ADRC concept, which made tremendous contributions to breaking the barrier between practice and theory. It was first introduced in the English literature by Gao *et al*. [20]. Whereafter, Gao [21] particularly presented a linear ADRC. Since PID controller evolved, ADRC adopts the core idea of PID error feedback control. The traditional PID control directly takes the difference between the reference given and the output feedback as the control signal, which leads to the contradiction between the quick response and the overshooting. ADRC technology does not depend on the precise mathematical model of the controlled object, nor does it need to know the model of external disturbance. It has strong robustness. The research of aircraft attitude control based on the ADRC technology is of great significance.

ESO has been widely used since it was first proposed by Han [22] because of the following two advantages: a) when the system dynamics is largely unknown, ESO can estimate the unknown dynamics and disturbances, and the upper bound of ESO estimation error monotonically de-

creases with the observer bandwidth; b) when the system dynamics is given, the dynamic system describing the estimation error is asymptotically stable [23]. ESO is the core part of ADRC, which mainly compensates the uncertain factors of unknown system. The purpose of feedback control is to suppress and eliminate the influence of various disturbances on the system output through negative feedback. Based on the idea of state observer [21,24], the combined effect of unmodeled dynamics and various disturbances is regarded as a new state-extended state, which is observed by output feedback. The ESO does not depend on the specific mathematical model of the system, it only depends on the order of the object [26].

By reviewing a large number of literatures, it is found that no (perhaps few) scholars have studied the attitude control of aircraft by using ADRC combined with back-stepping method so far. Because of this, in this paper, the back-stepping method is used to design the flight controller in the attitude control system of the aircraft, which is combined with the method of ADRC to compensate the uncertain influence, so that the attitude angle of the aircraft can track the desired trajectory target. In addition, compared with PID method, ADRC method has better control performance.

1.4. Research layout

The rest of this paper is structured as follows: Section 2 describes the non-linear aircraft model. Back-stepping ADRC is designed in Section 3. In Section 4, stability analysis of closed-loop dynamic is proofed, to be specific, stability of the ESO and stability of the ADRC. Simulation results are presented in Section 5 to testify the effectiveness of the proposed control method. Finally, Section 6 concludes the paper.

2. NON-LINEAR AIRCRAFT MODEL

The motion of an aircraft is usually represented in different coordinate systems [27]. The coordinate system constructed in this paper includes: S_g is treated as an inertial frame; S_h with its origin fixed in the aircraft at its center of gravity; S_w obtained from S_h by three successive rotations of χ, γ and μ (see Fig. 1); S_s obtained from S_w by rotation $-\beta$; and S_b obtained from S_s by rotation α (see Fig. 2). Certainly, the frame S_a is obtained by three successive rotations of ψ, θ, and ϕ as well. It is assumed that S_g and S_h have same orientation. Readers may obtain more matrix equations of various coordinate systems and aircraft motion equations by reference [28].

Consider the following non-linear aircraft system of the form. The inertial position coordinates $\begin{bmatrix} x & y & z \end{bmatrix}^T$ (superscript T denotes transposition) and force equations are

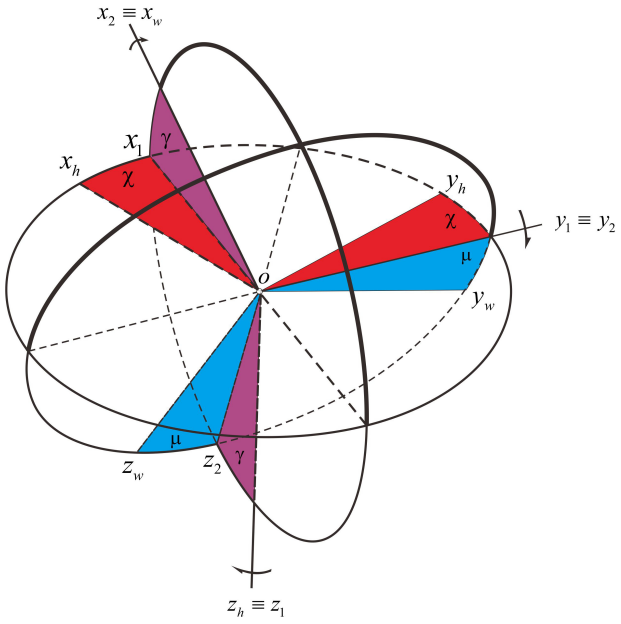

Fig. 1. System of rotations (χ, γ, μ) leading from local horizontal to wind axes.

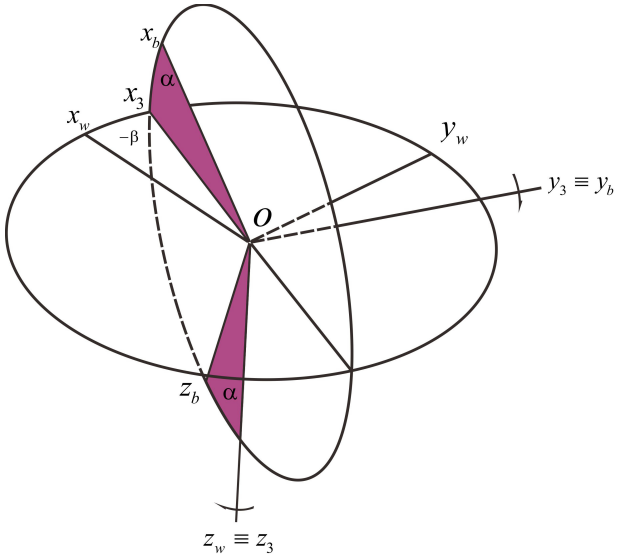

Fig. 2. System of rotations $(-\beta, \alpha)$ leading from wind axes to body axes.

described by

$$\begin{bmatrix} \dot{x} \\ \dot{y} \\ \dot{z} \end{bmatrix} = \begin{bmatrix} V\cos\chi\cos\gamma \\ V\sin\chi\cos\gamma \\ -V\sin\gamma \end{bmatrix}, \tag{1}$$

which is kinematical equation of aircraft centroid.

$$\begin{bmatrix} \dot{V} \\ \dot{\chi} \\ \dot{\gamma} \end{bmatrix} = \begin{bmatrix} -g\sin\gamma + (T_x\cos\alpha\cos\beta - D)/m \\ \hline [T_x(\sin\alpha\sin\mu - \cos\alpha\sin\beta\cos\mu) \\ -Q\cos\mu + L\sin\mu]/(mV\cos\gamma) \\ \hline [T_x(\cos\alpha\sin\beta\sin\mu - \sin\alpha\cos\mu) \\ +Q\sin\mu + L\cos\mu]/(mV) - g\cos\frac{\gamma}{V} \end{bmatrix}, \tag{2}$$

which is the dynamics of aircraft in the local horizontal system.

Next, yaw angle ψ, the pitch angle θ and roll angle ϕ also satisfy

$$\begin{bmatrix} \dot{\psi} \\ \dot{\theta} \\ \dot{\phi} \end{bmatrix} = \begin{bmatrix} (q\sin\phi + r\cos\phi)/\cos\theta \\ q\cos\phi - r\sin\phi \\ p + \tan\theta(q\sin\phi + r\cos\phi) \end{bmatrix}, \tag{3}$$

which is the kinematics equation of the aircraft rotating around the centroid.

The following equations are the angular motion equations of the aircraft in the airframe coordinate system:

$$\begin{bmatrix} \dot{p} \\ \dot{q} \\ \dot{r} \end{bmatrix} = \left(\frac{V}{V_0}\right)^2 \begin{bmatrix} l_\beta\beta + l_q q + l_r r + (l_{\beta\alpha}\beta \\ +l_{r\alpha})\Delta\alpha + l_p p + l_{\delta_a}\delta_a + l_{\delta_r}\delta_r \\ \hline m_\alpha\Delta\alpha + m_q q - m_{\dot{\alpha}} p\beta \\ +m_V\Delta V + m_{\dot{\alpha}}(g_0/V)\times \\ (\cos\theta\cos\phi - \cos\theta_0) + m_{\delta_e}\delta_e \\ \hline n_\beta\beta + n_r r + n_p p + n_{p\alpha} p\Delta\alpha \\ +n_q q + n_{\delta_a}\delta_a + n_{\delta_r}\delta_r \end{bmatrix} + \begin{bmatrix} -i_1 qr \\ i_2 pr \\ -i_3 pq \end{bmatrix}, \tag{4}$$

where $l_a = \frac{1}{2}\rho V_0^2 S_r l_1 \frac{\partial C_l}{\partial a}/I_x$, $m_a = \frac{1}{2}\rho V_0^2 S_r l_2 \frac{\partial C_m}{\partial a}/I_y$, and $n_a = \frac{1}{2}\rho V_0^2 S_r l_3 \frac{\partial C_n}{\partial a}/I_z$ $(a = \{\alpha, \beta, q, p, \cdots\})$ denote the aerodynamic derivatives computed at the trim condition (See Table 1 for details); and $i_1 = (I_z - I_y)/I_x$, $i_2 = (I_z - I_x)/I_y$, and $i_3 = (I_y - I_x)/I_z$. The factor $(V/V_0)^2$ in the rotational motion has been introduced because these parameters are proportional to the square of velocity.

By using the airframe coordinate system, wind coordinate system and local horizontal system, the geometric relation equation between aerodynamic angle, flight path angle and attitude angle is obtained

Table 1. The aerodynamic derivatives computed at the trim condition.

$l_\beta = \frac{1}{2}\rho V_0^2 S_r l_1 \frac{\partial C_l}{\partial \beta}/I_x$	$l_q = \frac{1}{2}\rho V_0^2 S_r l_1 \frac{\partial C_l}{\partial q}/I_x$
$l_r = \frac{1}{2}\rho V_0^2 S_r l_1 \frac{\partial C_l}{\partial r}/I_x$	$l_{\beta\alpha} = \frac{1}{2}\rho V_0^2 S_r l_1 \frac{\partial C_l}{\partial \beta\alpha}/I_x$
$l_{r\alpha} = \frac{1}{2}\rho V_0^2 S_r l_1 \frac{\partial C_l}{\partial r\alpha}/I_x$	$l_p = \frac{1}{2}\rho V_0^2 S_r l_1 \frac{\partial C_l}{\partial p}/I_x$
$l_{\delta_a} = \frac{1}{2}\rho V_0^2 S_r l_1 \frac{\partial C_l}{\partial \delta_a}/I_x$	$l_{\delta_r} = \frac{1}{2}\rho V_0^2 S_r l_1 \frac{\partial C_l}{\partial \delta_r}/I_x$
$m_\alpha = \frac{1}{2}\rho V_0^2 S_r l_2 \frac{\partial C_m}{\partial \alpha}/I_y$	$m_q = \frac{1}{2}\rho V_0^2 S_r l_2 \frac{\partial C_m}{\partial q}/I_y$
$m_{\dot{\alpha}} = \frac{1}{2}\rho V_0^2 S_r l_2 \frac{\partial C_m}{\partial \dot{\alpha}}/I_y$	$m_V = \frac{1}{2}\rho V_0^2 S_r l_2 \frac{\partial C_m}{\partial V}/I_y$
$m_{\delta_e} = \frac{1}{2}\rho V_0^2 S_r l_2 \frac{\partial C_m}{\partial \delta_e}/I_y$	$n_\beta = \frac{1}{2}\rho V_0^2 S_r l_3 \frac{\partial C_n}{\partial \beta}/I_z$
$n_r = \frac{1}{2}\rho V_0^2 S_r l_3 \frac{\partial C_n}{\partial r}/I_z$	$n_p = \frac{1}{2}\rho V_0^2 S_r l_3 \frac{\partial C_n}{\partial p}/I_z$
$n_{p\alpha} = \frac{1}{2}\rho V_0^2 S_r l_3 \frac{\partial C_n}{\partial p\alpha}/I_z$	$n_q = \frac{1}{2}\rho V_0^2 S_r l_3 \frac{\partial C_n}{\partial q}/I_z$
$n_{\delta_a} = \frac{1}{2}\rho V_0^2 S_r l_3 \frac{\partial C_n}{\partial \delta_a}/I_z$	$n_{\delta_r} = \frac{1}{2}\rho V_0^2 S_r l_3 \frac{\partial C_n}{\partial \delta_r}/I_z$

$$\begin{cases} \sin\gamma = \cos\alpha\cos\beta\sin\theta - (\sin\alpha\cos\beta\cos\phi \\ \qquad + \sin\beta\sin\phi)\cos\theta \\ \sin\chi\cos\gamma = \cos\alpha\cos\beta\sin\psi\cos\theta \\ \qquad - \sin\alpha\cos\beta(\cos\psi\sin\phi - \cos\phi\sin\psi\sin\theta) \\ \qquad + \sin\beta(\cos\psi\cos\phi + \sin\phi\sin\theta\sin\psi) \\ \sin\mu\cos\gamma = \cos\alpha\sin\beta\sin\theta - (\sin\alpha\sin\beta\cos\phi \\ \qquad - \cos\beta\sin\phi)\cos\theta, \end{cases} \tag{5}$$

$$\begin{bmatrix} \dot{\mu} \\ \dot{\alpha} \\ \dot{\beta} \end{bmatrix} = \begin{bmatrix} \sin\gamma + \cos\gamma\sin\mu\tan\beta & \cos\mu\tan\beta \\ \cos\gamma\sin\mu\sec\beta & -\cos\mu\sec\beta \\ \cos\gamma\cos\mu & -\sin\mu \end{bmatrix} \begin{bmatrix} \dot{\chi} \\ \dot{\gamma} \end{bmatrix} + \begin{bmatrix} \cos\alpha\sec\beta & 0 & \sin\alpha\sec\beta \\ -\cos\alpha\tan\beta & 1 & -\sin\alpha\tan\beta \\ \sin\alpha & 0 & -\cos\alpha \end{bmatrix} \begin{bmatrix} p \\ q \\ r \end{bmatrix}. \tag{6}$$

To force the output to track the reference signal Y_r is the control objective. The attitude angles $\begin{bmatrix} \psi & \theta & \phi \end{bmatrix}^T$ is the output vector which will be controlled and the deflection angle vector $\begin{bmatrix} \delta_a & \delta_r & \delta_e \end{bmatrix}^T$ is the control input.

The testability of the whole state is a strong assumption, for example, in aircraft system, this assumption is often not verified. Therefore, the following assumption is considered reasonably.

Hypothesis 1: In this paper it is hypothesized that just the states: attitude angle $[\psi\ \ \theta\ \ \phi]^T$, attitude angle velocity $[p\ \ q\ \ r]^T$ and aircraft speed V in the non-linear aircraft model (1)-(4) can be measured.

In order to describe the aircraft model explicitly, we define

$$\begin{cases} Y_1 \triangleq \begin{bmatrix} \psi & \theta & \phi \end{bmatrix}^T, \\ Y_2 \triangleq \begin{bmatrix} p & q & r \end{bmatrix}^T, \\ Y_3 \triangleq \begin{bmatrix} x & y & z \end{bmatrix}^T, \\ Y_4 \triangleq \begin{bmatrix} V & \chi & \gamma \end{bmatrix}^T, \\ U \triangleq \begin{bmatrix} \delta_a & \delta_r & \delta_e \end{bmatrix}^T. \end{cases} \tag{7}$$

Then the non-linear aircraft model (1)-(4) can be rewritten in the following:

$$\begin{cases} \dot{Y}_1 = G_1(Y_1)Y_2, \\ \dot{Y}_2 = G_2(Y_1,Y_2,Y_3,Y_4) + B(Y_1,Y_3,Y_4)U, \\ \dot{Y}_3 = G_3(Y_4), \\ \dot{Y}_4 = G_4(Y_1,Y_4), \end{cases} \tag{8}$$

where

$$G_1(Y_1) = \begin{bmatrix} 0 & \sin\phi/\cos\theta & \cos\phi/\cos\theta \\ 0 & \cos\phi & -\sin\phi \\ 1 & \tan\theta\sin\phi & \tan\phi\cos\phi \end{bmatrix}, \tag{9}$$

$$\begin{aligned} &G_2(Y_1,Y_2,Y_3,Y_4) \\ &= \begin{bmatrix} -i_1 qr \\ i_2 pr \\ -i_3 pq \end{bmatrix} + \frac{1}{2}\rho V^2 S_{\mathrm{r}} \mathcal{L} \\ &\quad \times \begin{bmatrix} [\frac{\partial C_l}{\partial \beta}\beta + \frac{\partial C_l}{\partial q}q + \frac{\partial C_l}{\partial r}r + (\frac{\partial C_l}{\partial \beta\alpha}\beta + \frac{\partial C_l}{\partial r\alpha})\Delta\alpha + \frac{\partial C_l}{\partial p}p]/I_x \\ [\frac{\partial C_m}{\partial \alpha}\Delta\alpha + \frac{\partial C_m}{\partial q}q - \frac{\partial C_m}{\partial \dot{\alpha}}p\beta + \frac{\partial C_m}{\partial V}\Delta V \\ + \frac{\partial C_m}{\partial \dot{\alpha}}(g_0/V) \times (\cos\theta\cos\phi - \cos\theta_0)]/I_y \\ [\frac{\partial C_n}{\partial \beta}\beta + \frac{\partial C_n}{\partial r}r + \frac{\partial C_n}{\partial p}p + \frac{\partial C_n}{\partial p\alpha}p\Delta\alpha + \frac{\partial C_n}{\partial q}q]/I_z \end{bmatrix}, \end{aligned} \tag{10}$$

where $\mathcal{L} = \begin{bmatrix} l_1 & l_2 & l_3 \end{bmatrix}^T$ are the reference lateral and longitudinal lengths, respectively;

$$G_3(Y_4) = \begin{bmatrix} V\cos\chi\cos\gamma \\ V\sin\chi\cos\gamma \\ -V\sin\gamma \end{bmatrix}, \tag{11}$$

$$G_4(Y_1,Y_4) = \begin{bmatrix} -g\sin\gamma + (T_x\cos\alpha\cos\beta - D)/m \\ \{T_x(\sin\alpha\sin\mu - \cos\alpha\sin\beta\cos\mu) \\ -Q\cos\mu + L\sin\mu\}/(mV\cos\gamma) \\ \{T_x(\cos\alpha\sin\beta\sin\mu - \sin\alpha\cos\mu) \\ +Q\sin\mu + L\cos\mu\}/(mV) - g\cos\frac{\gamma}{V} \end{bmatrix}, \tag{12}$$

$$B(Y_1,Y_3,Y_4) = \frac{1}{2}\rho V^2 S_{\mathrm{r}} \mathcal{L} \times \begin{bmatrix} \frac{\frac{\partial C_l}{\partial \delta_a}}{I_x} & \frac{\frac{\partial C_l}{\partial \delta_r}}{I_x} & 0 \\ 0 & 0 & \frac{\frac{\partial C_m}{\partial \delta_e}}{I_y} \\ \frac{\frac{\partial C_n}{\partial \delta_a}}{I_z} & \frac{\frac{\partial C_n}{\partial \delta_r}}{I_z} & 0 \end{bmatrix}. \tag{13}$$

The uncertainty, which exists in the atmospheric moment coefficients $\frac{\partial C_l}{\partial *}$, $\frac{\partial C_m}{\partial *}$, $\frac{\partial C_n}{\partial *}$, is the main problem in system (8). The moment coefficients rely on the Mach number M_a, which is also a variable related to the states Y_1, Y_2, Y_3 and Y_4. But, the coefficients $\frac{\partial C_l}{\partial *}$, $\frac{\partial C_m}{\partial *}$ and $\frac{\partial C_n}{\partial *}$, cannot be accurately determined in the actual aircraft system; the model uncertainty always exists in the atmospheric moment coefficient of aircraft. Hence, the structure of the system (8) poses a particular difficulty because G_2 and B are unknown due to the dynamic uncertainties in the atmospheric moment coefficient, which makes the control design more complex. In order to solve this problem, a new variable $H(t)$ will be introduced and defined as

$$H(t) = G_2(Y_1,Y_2,Y_3,Y_4) + B(Y_1,Y_3,Y_4)U - B_0 U, \tag{14}$$

where B_0 is defined as

$$B_0 = \frac{1}{2}\rho V^2 S_{\mathrm{r}} \mathcal{L} \Phi|_{M_a=const}, \tag{15}$$

where $\Phi|_{M_a=const}$ is defined as

$$\Phi|_{M_a=const} = \begin{bmatrix} \frac{\partial C_l}{\partial \delta_a}/I_x & \frac{\partial C_l}{\partial \delta_r}/I_x & 0 \\ 0 & 0 & \frac{\partial C_m}{\partial \delta_e}/I_y \\ \frac{\partial C_n}{\partial \delta_a}/I_z & \frac{\partial C_n}{\partial \delta_r}/I_z & 0 \end{bmatrix}|_{M_a=const}.$$

It is can be obtained the coefficients $\frac{\partial C_l}{\partial \delta_a}$, $\frac{\partial C_l}{\partial \delta_r}$, $\frac{\partial C_m}{\partial \delta_e}$, $\frac{\partial C_n}{\partial \delta_a}$, and $\frac{\partial C_n}{\partial \delta_r}$ by choosing the suitable constant Maher number M_a. These coefficients can be utilized as the certain part B_0 and decompose the uncertain part into variable $H(t)$. By this way, the dynamic uncertainty existing in (8) can be attributed to the total uncertainty $H(t)$, thus reducing the complexity of the control design. Therefore,

system (8) can be redescribed as

$$\dot{Y}_1 = G_1(Y_1)Y_2, \tag{16a}$$
$$\dot{Y}_2 = H(t) + B_0U(t). \tag{16b}$$

The aircraft system (8) can be simplified to a second-order system by introducing the new state variable $H(t)$, thus directly reducing the complexity of the control design. Nevertheless, due to the loss of Y_3 and Y_4, $H(t)$ is unknown to us, and can be regarded as the uncertainties which contains the information of Y_3 and Y_4.

Remark 1: The introduction of $H(t)$ is based on strict mathematical logic. In (14), $H(t) = G_2(Y_1,Y_2,Y_3,Y_4) + B(Y_1,Y_3,Y_4)U - B_0U$, combining formula (7) and system (8) shows that $H(t)$ is derivable. Furthermore, please refer to Table 1 in the text for the aerodynamic derivative in the aircraft system.

Uncertain factors in $H(t)$ include density changes caused by airflow changes, pressure changes caused by airflow changes, changes in outside temperature during aircraft flight, angle of attack, and airflow speed, and so on.

Remark 2: From defining of B_0, we can see that $B_0 = \frac{1}{2}\rho V^2 S_r \mathcal{L}\Phi|_{M_a=const}$, where ρ is air density, $\rho > 0$; V is the velocity of aircraft, $V > 0$; S_r is the reference area, $S_r > 0$; $\mathcal{L}$ is the reference lateral or longitudinal lengths, $\mathcal{L} > 0$; if $\Phi|_{M_a=const}$ is invertible, then B_0 is invertible. In fact, $\Phi|_{M_a=const}$ is invertible. C_l, C_m, C_n are moment coefficients of roll, pitch and yaw, respectively; Obviously, C_l, C_m, C_n all can be derived, and the derivative functions are not zero. In short, $\Phi|_{M_a=const}$ is reversible, and then B_0 is reversible.

3. BACK-STEPPING ADRC DESIGN

3.1. Back-stepping procedure

The actual state is Y_i, the desired state is defined as $Y_{r,i}$, and the state error is defined as e_i. Hence $e_i = Y_i - Y_{r,i}$. Starting from defining tracking error e_1

$$e_1 = Y_1 - Y_{r,1}, \tag{17}$$

with $Y_{r,1} = Y_r$ being the reference value for $Y_{r,1}$, it is can be obtained the derivative of e_1

$$\dot{e}_1 = \dot{Y}_1 - \dot{Y}_r = G_1(Y_1)Y_2 - \dot{Y}_r. \tag{18}$$

According to the principle of back-stepping, the former subsystem can be stabilized by virtual control of the latter subsystem.

Choosing $\mathcal{V} = \frac{1}{2}e_1^2$ Lyapunov function candidate, we obtain

$$\dot{\mathcal{V}} = e_1^T\dot{e}_1 = e_1^T[G_1(Y_1)Y_2 - \dot{Y}_r]. \tag{19}$$

To obtain $\dot{\mathcal{V}} < 0$, let $Y_2 = Y_{r,2} + e_2 = \dot{Y}_{r,1} - \Pi e_1 + e_2$, then $\dot{\mathcal{V}} = e_1^T[G_1(Y_1)(\dot{Y}_{r,1} - \Pi e_1 + e_2) - \dot{Y}_r]$. Y_2 is considered as a virtual control input utilized to impose the following desired dynamics:

$$\dot{e}_1 = -\Pi e_1 = -\text{diag}\begin{bmatrix} \pi_1 & \pi_2 & \pi_3 \end{bmatrix} e_1. \tag{20}$$

For guaranteeing the asymptotic stability of (18), the design matrix Π is selected as $\pi_i > 0$, $i = 1,2,3$. After calculation, if $Y_2 = G_1^{-1}(Y_1)(\dot{Y}_r - \Pi e_1)$, then $\dot{\mathcal{V}} < 0$. Hence combining (17) and (18), the solution can be obtained:

$$Y_{r,2} = G_1^{-1}(Y_1)(\dot{Y}_r - \Pi e_1). \tag{21}$$

Remark 3: In (9), when $\theta = \pm 90^\circ$, $G_1(Y_1)$ is a singular value, which limits the control range of pitch angle. For the sake of simplicity, the pitch angle control is considered under the condition of $-90^\circ < \theta < 90^\circ$, which means that $G_1(Y_1)$ is nonsingular in this paper. In practice, pitch angle of the vertical takeoff and landing aircraft system must be 90° but there is no such requirement in horizontal take-off aircraft systems. Therefore, the control design under the constraint of $-90^\circ < \theta < 90^\circ$ can be reasonably applied to practical horizontal take-off aircraft systems.

3.2. Extended state observer design

ADRC is utilized to control the aircraft system by dealing with modeling errors and structural uncertainties in this paper. Before all, an ESO supplies an estimation of the internal kinematics of the aircraft system.

A nonlinear continuous ESO is designed to estimate the uncertainty $H(t)$ in the control law. An augmented state Y_5 is considered as the uncertainties $H(t)$, thus, we can rewrite the sub-plant (16b) as follows:

$$\begin{cases} \dot{Y}_2 = Y_5 + B_0U(t), \\ \dot{Y}_5 = h(t), \\ X = Y_2, \end{cases} \tag{22}$$

where $Y_2 = X$; the derivative of the uncertainties $H(t)$ is $h(t)$ which is uncertain as well. Then the second-order ESO for systems (22) is designed as

$$\begin{cases} \varepsilon_1 = Z_1 - Y_2, \\ \dot{Z}_1 = Z_2 + B_0U(t) - \lambda_1\varepsilon_1, \\ \dot{Z}_2 = -\lambda_2 \text{fal}(\varepsilon_1,\sigma,\delta), \\ \hat{X} = Z_1, \end{cases} \tag{23}$$

where ε_1 is the estimation error of the ESO, $\begin{bmatrix} Z_1 & Z_2 \end{bmatrix}^T$ is the observed state variables for $\begin{bmatrix} Y_2 & Y_5 \end{bmatrix}^T$, $\hat{X}$ is the observed output for X, and $\begin{bmatrix} \lambda_1 & \lambda_2 \end{bmatrix}^T$ is the observer gain vector. The observer gains are chosen such that the characteristic polynomial $s^2 + \lambda_1 s + \lambda_2$ is Hurwitz. In order to optimize simplicity, all the observer poles are placed

at $-\omega_o$. It results in the characteristic polynomial of (23) to be

$$\lambda_o(s) = s^2 + \lambda_1 s + \lambda_2 = (s+\omega_o)^2, \tag{24}$$

where ω_o is denoted as the bandwidth of the observer and $\begin{bmatrix} \lambda_1 & \lambda_2 \end{bmatrix}^T = \begin{bmatrix} 2\omega_o & \omega_o^2 \end{bmatrix}^T$.

We define the function fal$(\cdot)$ as

$$\text{fal}(\varepsilon_1, \sigma, \delta) = \begin{bmatrix} \text{fal}_1(\varepsilon_1, \sigma, \delta) \\ \text{fal}_2(\varepsilon_1, \sigma, \delta) \\ \text{fal}_3(\varepsilon_1, \sigma, \delta) \end{bmatrix}, \tag{25}$$

where

$$\text{fal}_i(\varepsilon_1, \sigma, \delta) = \begin{cases} \dfrac{\varepsilon_{1i}}{\delta^{1-\sigma}}, & |\varepsilon_{1i}| \le \delta, \\ |\varepsilon_{1i}|^{\sigma}\text{sign}(\varepsilon_{1i}), & |\varepsilon_{1i}| > \delta, \end{cases} \tag{26}$$

where ε_{1i} is the ith component of vector ε_1, $0 < \sigma < 1$, $\delta > 0$. For appropriate values of λ_1, λ_2, σ, δ the observer output Z_2 is approximate to $H(t)$ and Z_1 is approximate to Y_2.

3.3. ADRC design

With the ESO properly being designed, the control law is acquired by

$$U(t) = B_0^{-1}(-Z_2 + U_0). \tag{27}$$

Ignoring the estimation error in Z_2, the plant (16b) is reduced a unit gain integrator

$$\dot{Y}_2 = (H(t) - Z_2) + U_0 \approx U_0, \tag{28}$$

where U_0 is output of the state error feedback. It is easily controlled by a proportional controller, which is acquired by

$$U_0 = K_p(Y_{r,2} - Z_1), \tag{29}$$

where $K_p > 0$ is the proportional constant of the proportional controller. Then the control law (27) can be rewritten as follows:

$$U(t) = B_0^{-1}[-Z_2 + K_p(Y_{r,2} - Z_1)]. \tag{30}$$

Remark 4: By calculating (21) we can obtain the virtual control input $Y_{r,2}$, but which may not be obtained without difficulty because of $\dot{Y}_r$. Here, in order to acquire $\dot{Y}_r$, the TD [29] is introduced. Here's a brief design of TD which is utilized for tracking reference signal.

$$\begin{cases} \dot{\chi}_1 = \chi_2, \\ \dot{\chi}_2 = -\kappa_1 R^2(\chi_1 - Y_r) - \kappa_2 R\chi_2, \end{cases} \tag{31}$$

where χ_1 and χ_2 are the state variables of TD, $\kappa_1 > 0, \kappa_2 > 0$ are constants that denote the maximum actuation available in the system; and $R > 0$ is the tuning parameter.

Lemma 1 [25]**:** Suppose that $\kappa_1 > 0, \kappa_2 > 0$ and $Y_r : [0,\infty) \to R$ is a function satisfying $\sup_{t\in[0,\infty)} (|Y_r| + |\dot{Y}_r|) = M_1 < \infty$ for constant $M_1 > 0$. Then the linear tracking differentiator (31) is convergent in the sense that, for $\forall a > 0$,

$$\begin{cases} \lim\limits_{R\to\infty} |\chi_1 - Y_r| = 0, \\ \lim\limits_{R\to\infty} |\chi_2 - \dot{Y}_r| = 0, \end{cases}$$

uniformly for $t \in [a,\infty)$.

According to Lemma1, the TD states χ_1, χ_2 will be as fast as possible approximate to Y_r, $\dot{Y}_r$, respectively. Xia, Y. Q. etc, has demonstrated the benefits of this tracking method, for more details, please refer to [29,30]. In [24], there is further explanations of TD. Hence $\dot{Y}_r$ can be acquired with the help of designing of TD for Y_r.

Remark 5: The signum function in (26) are defined as

$$\text{sign}(x) = \begin{cases} 1, & x > 0, \\ 0, & x = 0, \\ -1, & x < 0. \end{cases}$$

A general way to avoid chattering effect is a smooth approximation of the signum function, by replacing $sign(x)$ by $sat(x)$ we have

$$\text{sat}(\frac{x}{\xi}) = \begin{cases} \dfrac{1}{\xi}x, & \text{if } \|x\| \le \xi, \\ \text{sign}(x), & \text{if } \|x\| > \xi, \end{cases} \tag{32}$$

where ξ is small boundary layer thickness.

Remark 6: Obviously, once the values of the state variables Y_1, Y_2 are measured based on the hypothesis (1), $Y_{r,2}$ can be obtained by computing by (17)-(21), $\dot{Y}_r$ can be acquired by designing TD for Y_r, Z_2 can be gained by (23), now that the controller (30) can be calculated completely.

4. STABILITY ANALYSIS OF CLOSED-LOOP DYNAMIC

The stability for the estimation error of ESO and the convergence closed-loop tracking error of the ADRC is shown hereinafter.

Definition 1 [31]**:** Study the non-linear system, $\dot{x} = f(x,u)$, $y = h(x)$ with x being a state vector, u being the input vector and y being the output vector. If $\forall x(t_0) = x_0$, the solution is UUB, there exists $\varepsilon > 0$ and $T(\varepsilon, x_0)$, such that $\|x(t)\| < \varepsilon$, $\forall t \ge t_0 + T$.

Lemma 2 (Barbashin-Krasovski Theorem) [31,35]**:** Let $x = 0$ be an equilibrium point for system

$$\dot{x} = f(x), f(0), x \in \mathbb{R}^n, \tag{33}$$

where $f : U \to \mathbb{R}^n$ is a continuously differentiable on an open neighborhood U of the origin $x = 0$ in $\mathbb{R}^n$.

Let $V(x):\mathbb{R}^n\to\mathbb{R}$ be a continuously differentiable function such that

$$\begin{cases} V(0)=0,\ \ V(x)>0,\ \ \forall x\neq 0,\\ \|x\|\to\infty\Rightarrow V(x)\to\infty,\\ \dot{V}(x)<0,\ \ \forall x\neq 0. \end{cases}$$

Then $x=0$ is globally asymptotically stable.

Lemma 3 [37]**:** If a Lyapunov description of finite-time stability can be given as

$$\dot{L}(x)+\tau_1 L(x)+\tau_2 L^{\mu}(x)\leq 0,$$
$$\tau_1>0,\ \tau_2>0,\ 0<\mu<1,$$

and the settling time can be acquired by

$$T\leq\frac{1}{\tau_1(1-\mu)}\ln\frac{\tau_1 L^{1-\mu}(x_0)+\tau_2}{\tau_2}$$

such that the equilibrium point $x=0$ is globally finite-time stable for any given initial condition $x(0)=x_0\ \forall t>T$.

Lemma 4 [36]**:** Let $x=0$ be an equilibrium point for system (33). Let $V(x):U\to\mathbb{R}$ is a continuously differentiable function, real numbers $c>0$ and $\zeta\in(0,1)$, and an open neighborhood $U_0\subset U$ of the origin such that

$$\begin{cases} V(0)=0,\ \text{ and }\ V(x)>0,\ \ \forall x\neq 0,\\ \dot{V}(x)+c(V(x))^{\zeta}\leq 0,\ \ x\in U_0\backslash\{0\}. \end{cases}$$

Then the origin $x=0$ is a finite-time stable equilibrium point of system (33). In addition, the finite setting T satisfies that $T\leq V^{1-\zeta}(x(0))/(c(1-\zeta))$.

Lemma 5 [38]**:** Let $x=0$ be an equilibrium point for system (33). Suppose that all the conditions of Lemma 2 and Lemma 4 are satisfied, the origin $x=0$ is a globally finite-time stable equilibrium point.

Lemma 6 [39]**:** The autonomous scalar system

$$\dot{x}(t)=-csign^{\zeta}(x(t))$$

is globally finite-time stable, where $sign^{\zeta}(x)=|x|^{\zeta}sign(x)$, c is a positive real number, and $\zeta\in(0,1)$. For arbitrary initial state value $x(t_0)$, the finite settling time t_s satisfies $t_s=|x(t_0)|^{1-\zeta}/(c(1-\zeta))$.

4.1. Astringency of the ESO

In order to test the stability of the CLS, an expression of observer error dynamics must be established.

Defining the observer error

$$\begin{cases} \varepsilon_1=Z_1-Y_2,\\ \varepsilon_2=Z_2-Y_5=Z_2-H(t). \end{cases}\tag{34}$$

Theorem 1: Here the new subsystem (22) and ESO (23) are considered, hypothesize that $h(t)$ is bounded, there exist a positive constant $\rho_i, i=1,2$ and a finite time $T>0$ such that $|\varepsilon_i|\leq\rho_i,\forall t\geq T>0$ and $\omega_o>0$; and there exist the parameters λ_1, λ_2, σ and δ such that Z_1, Z_2 astringe to Y_2, $H(t)$ respectively.

Proof: On the basis of (22), (23) and (34), the observer error kinematics are denoted as

$$\begin{aligned} \dot{\varepsilon}_1&=\dot{Z}_1-\dot{Y}_2\\ &=Z_2+B_0U(t)-\lambda_1\varepsilon_1-Y_5-B_0U(t)\\ &=Z_2-H(t)-\lambda_1\varepsilon_1\\ &=\varepsilon_2-\lambda_1\varepsilon_1,\\ \dot{\varepsilon}_2&=\dot{Z}_2-\dot{H}(t)\\ &=-\lambda_2\mathrm{fal}(\varepsilon_1,\sigma,\delta)-h(t). \end{aligned}\tag{35}$$

The observer estimation error ε_i is scaled by ω_o^{i-1}, in other words, $\xi_i=\frac{\varepsilon_i}{\omega_o^{i-1}}$, $i=1,2$. Then, (35) can be rewritten as

$$\dot{\xi}=\omega_o A_\xi\xi+B_\xi\frac{h(t)}{\omega_o},\tag{36}$$

where $A_\xi=\begin{bmatrix}-2&1\\-1&0\end{bmatrix}$, $B_\xi=\begin{bmatrix}0\\1\end{bmatrix}$.

Solving (36), it can be obtained

$$\xi=e^{\omega_o A_\xi t}\xi(0)+\int_0^t e^{\omega_o A_\xi(t-\tau)}B_\xi\frac{h(\tau)}{\omega_o^2}d\tau.\tag{37}$$

Let

$$p=\int_0^t e^{\omega_o A_\xi(t-\tau)}B_\xi\frac{h(\tau)}{\omega_o^2}d\tau.\tag{38}$$

First, one must consider the positive and negative situation of $e^{\omega_o A_\xi(t-\tau)}B_\xi$, if one wants to prove that (35) is true.

From $A_\xi=\begin{bmatrix}-2&1\\-1&0\end{bmatrix}$, solving the eigenvalues of A_ξ, then $|A_\xi-\lambda E|=0$, $\lambda^2+2\lambda+1=(\lambda+1)^2=0$, Matrix A_ξ has two equal eigenvalues: $\lambda_{1,2}=-1$. Furthermore $(A_\xi-\lambda E)=(A_\xi+E)=\begin{bmatrix}-1&1\\-1&1\end{bmatrix}$, $(A_\xi+E)^2=\begin{bmatrix}0&0\\0&0\end{bmatrix}$. Utilize the following formula to solve the fundamental matrix of $e^{\omega_o A_\xi(t-\tau)}$.

$$expAt=e^{\lambda t}exp(A-\lambda E)t=e^{\lambda t}\sum_{i=0}^{n-1}\frac{t^i}{i!}(A-\lambda E)^i.\tag{39}$$

In order to facilitate the calculation, let $x=\omega_o(t-\tau)$, obviously, $x>0$.

$$\begin{aligned} &e^{\omega_o A_\xi(t-\tau)}=e^{A_\xi x}\\ &=e^{-x}\left[E+x(A+E)+\frac{x^2}{2}(A+E)^2\right]\\ &=e^{-x}\left\{\begin{bmatrix}1&0\\0&1\end{bmatrix}+\begin{bmatrix}-x&x\\-x&x\end{bmatrix}\right\} \end{aligned}$$

$$= e^{-x}\begin{bmatrix} -x+1 & x \\ -x & x+1 \end{bmatrix}. \tag{40}$$

On the basis of $B_\xi = \begin{bmatrix} 0 & 1 \end{bmatrix}^T$, it can be further obtained

$$e^{\omega_o A_\xi (t-\tau)} B_\xi = e^x \begin{bmatrix} x \\ x+1 \end{bmatrix}. \tag{41}$$

It is apparent to know $(e^{\omega_o A_\xi (t-\tau)} B_\xi)_i > 0, i = 1,2$. According to $|h(t)| \le \delta$, the rigorous proof will be shown as follows:

$$\begin{aligned} p_i &= \int_0^t \left(e^{\omega_o A_\xi (t-\tau)} B_\xi\right)_i \frac{h(\tau)}{\omega_o} d\tau \\ &= \frac{1}{\omega_o}\int_0^t \left(e^{\omega_o A_\xi (t-\tau)} B_\xi\right)_i h(\tau) d\tau \\ &\le \frac{\delta}{\omega_o^2}\int_0^t \left(e^{\omega_o A_\xi (t-\tau)} B_\xi\right)_i d\tau \\ &= \frac{\delta}{\omega_o}(e^{\omega_o A_\xi t})_i \int_0^t \left(e^{-\omega_o A_\xi \tau} B_\xi\right)_i d\tau \\ &= \frac{\delta}{\omega_o}(e^{\omega_o A_\xi t})_i \left(\frac{1}{-\omega_o A_\xi}\right)_i \left(e^{-\omega_o A_\xi \tau} B_\xi\right)_i \Big|_0^t \\ &= \frac{\delta}{\omega_o}(e^{\omega_o A_\xi t})_i \left(\frac{1}{-\omega_o A_\xi}\right)_i \left(e^{-\omega_o A_\xi t} B_\xi - B_\xi\right)_i \\ &= \frac{\delta}{\omega_o^2}\left(\frac{1}{-A_\xi}\right)_i \left(B_\xi - e^{\omega_o A_\xi t} B_\xi\right)_i \\ &= \frac{\delta}{\omega_o^2}\left[(-A_\xi^{-1} B_\xi)_i + (A_\xi^{-1} e^{\omega_o A_\xi t} B_\xi)_i\right],\ i = 1,2. \end{aligned} \tag{42}$$

Hence

$$|p_i| \le \frac{\delta}{\omega_o^2}\left[|(-A_\xi^{-1} B_\xi)|_i + |(A_\xi^{-1} e^{\omega_o A_\xi t} B_\xi)|_i\right],\ i = 1,2. \tag{43}$$

Since $A_\xi^{-1} = \begin{bmatrix} 0 & -1 \\ 1 & -2 \end{bmatrix}$, it can be acquired

$$\left|\left(A_\xi^{-1} B_\xi\right)_i\right| = \begin{cases} 1|_{i=1}, \\ 2|_{i=2}. \end{cases} \tag{44}$$

Since A_ε is Hurwitz, there is a finite time $T > 0$ such that

$$\left|\left[e^{\omega_o A_\xi t}\right]_{ij}\right| \le \frac{1}{\omega_o^2},\ \forall t \ge T,\ i,j = 1,2. \tag{45}$$

Therefore

$$\left|\left[e^{\omega_o A_\xi t}\right]_{i}\right| \le \frac{1}{\omega_o^2},\ \forall t \ge T,\ i,j = 1,2. \tag{46}$$

From (37), it can be acquired

$$\left|\xi_i\right| \le \left|\left[e^{\omega_o A_\xi t}\xi(0)\right]_i\right| + \left|p_i\right|. \tag{47}$$

Let $\varepsilon_{sum}(0) = \varepsilon_1(0) + \frac{|\varepsilon_2(0)|}{\omega_o}$. In light of $\xi_i = (\varepsilon_i)/(\omega_o^{i-1})$, it can be obtained

$$\left|\varepsilon_i\right| \le \left|\frac{\varepsilon_{sum}(0)}{\omega_o^2}\right| + \frac{2\delta}{\omega_o^{3-i}} + \frac{4\delta}{\omega_o^{5-i}} = \rho_i,\ \forall t \ge T,\ i = 1,2. \tag{48}$$

So far, the finite time convergence is proved.

Next, the stability of ESO has been acquired by choosing suitable parameters λ_1 and λ_2 [32]. $\dot{\varepsilon} = [\dot{\varepsilon}_1, \dot{\varepsilon}_2]^T = 0$ when the ESO is stable, and then one can write the estimation error as

$$\begin{bmatrix} \varepsilon_2 \\ \mathrm{fal}(\varepsilon_1, \sigma, \delta) \end{bmatrix} = \begin{bmatrix} \lambda_1 \varepsilon_1 \\ -h(t)/\lambda_2 \end{bmatrix}. \tag{49}$$

If $|\varepsilon_{1i}| > \delta$, calculating (49) and considering (26), it can be obtained

$$\begin{vmatrix} \varepsilon_{1i} \\ \varepsilon_{2i} \end{vmatrix} = \begin{bmatrix} \sqrt[\sigma]{|h_i(t)/\lambda_2|} \\ \lambda_1 \sqrt[\sigma]{|h_i(t)/\lambda_2|} \end{bmatrix}. \tag{50}$$

If $|\varepsilon_{1i}| \le \delta$, one can write the estimation errors as

$$\begin{vmatrix} \varepsilon_{1i} \\ \varepsilon_{2i} \end{vmatrix} = \frac{1}{\lambda_2}\begin{bmatrix} |h_i(t)\delta^{1-\sigma}| \\ \lambda_1 |h_i(t)\delta^{1-\sigma}| \end{bmatrix}, \tag{51}$$

with $h_i(t)$ being the ith component of vector $h(t)$.

It can be seen from the above analysis that whether it is $|\varepsilon_{1i}| > \delta$ or $|\varepsilon_{1i}| \le \delta$, the estimation errors ε_1 and ε_2 depend on the observer gains λ_1, λ_2, σ and δ. By adjusting these parameters properly, the estimation errors of the observer are small enough, so that the system state Y_2 and extended state Y_5 can be observed effectively by ESO, that is, the estimated states Z_1, Z_2 will converge to the actual state of Y_2 and $H(t)$, respectively. $\lambda_1, \lambda_2 \in (0, \infty)$ and $\sigma, \delta \in (0,1)$ are the basic criterion for parameter selection. Furthermore, although $h_i(t)$ is unknown, we can choose a suitable λ_2 large enough to make $|h(t)/\lambda_2|$ small enough. Thus, λ_1 should be small enough such that the estimation error ε_2 is as small as possible. Additionally, the smaller σ is, the smaller the steady-state estimation error is [30]. The proof is completed. □

Remark 7: It is very crucially to select the ESO parameter which decides the stability of the observer. Additionally, under the practical circumstance, information which is unavailable on the internal states of the plants are provided by state observers. They are also used as noise filters. Hence, it is very important to select parameters to provide the appropriate bandwidth. For more information on parameter optimization of ESO, see [21,22,33].

4.2. Stability of the ADRC

Let $e_i = Y_i - Y_{r,i}, i = 1,2$.

Theorem 2: With the ESO obtained by (23), the trajectory of the CLS (16) can converge into a residual set of the reference trajectory in finite time with the control law (30); in addition, e_1 is UUB by which Y_1 tracking the reference Y_r is guaranteed.

Proof: From (30), it can be obtained

$$U(t) = B_0^{-1}\{-Z_2 + K_p[G_1^{-1}(Y_1)(\dot{Y}_r - K_1 e_1) - Z_1]\}. \tag{52}$$

According to the principle of back-stepping method, each virtual input is designed to make each subsystem stable, and then the stable input of the system can be obtained.

The convergence of ADRC is proven by considering the Lyapunov function as

$$\mathscr{L} = \frac{1}{2K_p} Z_1^T Z_1. \tag{53}$$

Then, with (52), the time derivative of $\mathscr{L}$ can be calculated by

$$\begin{aligned}
\dot{\mathscr{L}} &= K_p^{-1} Z_1^T \dot{Z}_1 \\
&= K_p^{-1} Z_1^T (Z_2 + B_0 U(t) - \lambda_1 \varepsilon_1) \\
&= K_p^{-1} Z_1^T (\varepsilon_2 + H(t) + B_0 U(t) - \lambda_1 \varepsilon_1) \\
&= K_p^{-1} Z_1^T [H(t) + B_0 U(t)] \\
&= K_p^{-1} Z_1^T \{H(t) - Z_2 + K_p[G_1^{-1}(Y_1)(\dot{Y}_r - \Pi e_1) - Z_1]\} \\
&\le -\|Z_1\|^2 + K_p^{-1} Z_1^T (H(t) - Z_2) \\
&\quad + Z_1^T [G_1^{-1}(Y_1)(\dot{Y}_r - \Pi e_1)].
\end{aligned} \tag{54}$$

According to Theorem 1, we know that Z_2 astringe to $H(t)$, $\|H(t) - Z_2\| \longrightarrow 0$ it can be obtained

$$\dot{\mathscr{L}} \le -\|Z_1\|^2 + Z_1^T [G_1^{-1}(Y_1)(\dot{Y}_r - \Pi e_1)]. \tag{55}$$

Substituting (20) and (21) into (55), we obtain

$$\begin{aligned}
\dot{\mathscr{L}} &\le -\|Z_1^2\| + \|Z_1^T [G_1^{-1}(Y_1)(G_1(Y_1)Y_2 - \dot{e}_1 + \dot{e}_1)] \\
&= -\|Z_1\|^2 + Z_1^T Y_2.
\end{aligned} \tag{56}$$

Substituting (34) into (56), we acquire

$$\begin{aligned}
\dot{\mathscr{L}} &\le -\|Z_1\|^2 + \|Z_1\|^2 - \|Z_1^T \varepsilon_1\| \\
&\le -\|Z_1^T \varepsilon_1)\| < 0.
\end{aligned} \tag{57}$$

Hence, the trajectory of the CLS (15) can converge into a residual set of the reference trajectory in finite time with the control law (30).

Next, Consider the Lyapunov function candidate

$$\mathcal{V} = \frac{1}{2} e_1^T e_1. \tag{58}$$

Taking the derivative of (58)

$$\begin{aligned}
\dot{\mathcal{V}} &= e_1^T \dot{e}_1 \\
&= e_1^T (\dot{Y}_1 - \dot{Y}_r) \\
&= e_1^T (G_1(Y_1) Y_2 - \dot{Y}_r) \\
&= e_1^T [G_1(Y_1)(e_2 + Y_{r,2}) - \dot{Y}_r] \\
&= e_1^T [G_1(Y_1)(e_2 + G_1^{-1}(Y_1)(\dot{Y}_r - \Pi e_1) - \dot{Y}_r] \\
&= e_1^T (G_1(Y_1) e_2 - \Pi e_1) \\
&= -e_1^T \Pi e_1 + e_1^T G_1(Y_1) e_2 \\
&= -\sum_{i=1}^{3} \pi_i e_{1i}^2 + e_1^T G_1(Y_1) e_2,
\end{aligned} \tag{59}$$

with e_{1i} being the ith component of e_1. If e_2 is bounded, the positive π_i is selected large enough such that it can be acquired $\dot{\mathcal{V}} < 0$.

Next, we are going to prove that e_2 is bounded. Consider (30), it can be rewritten as follows:

$$U(t) = -B_0^{-1}[K_p(e_2 + \varepsilon_1) + H(t) + \varepsilon_2]. \tag{60}$$

It follows that

$$\dot{e}_2 = -K_p(e_2 + \varepsilon_1) - \varepsilon_2. \tag{61}$$

Let $C(t) = -K_p \varepsilon_1 - \varepsilon_2$, according to [33], it can be acquired $|C(t)| \le M_2$ where M_2 is positive constant.

Solving (61), one has

$$\begin{aligned}
e_2 &= e_2^{-K_p t} e_2(0) + \int_0^t C(t) e_2^{\int_t^\tau K_p ds} d\tau \\
&\le e_2(0) + M_2 \int_0^t e_2^{K_p(\tau - t)} d\tau \\
&= e_2(0) + M_2 e_2^{-K_p t} \int_0^t e_2^{K_p \tau} d\tau \\
&= e_2(0) + M_2 e_2^{-K_p t} (e_2^{K_p t} - 1) \\
&= e_2(0) + M_2 (1 - e_2^{-K_p t})/K_p.
\end{aligned} \tag{62}$$

Since $K_p > 0$, obviously, $e_2 < e_2(0) + M_2/K_p$. Hence, e_2 is bounded. Then $\dot{\mathcal{V}} < 0$ when positive π_i is selected large enough. In addition, e_1 is UUB by guaranteeing the Y_1 tracking the reference Y_r. The proof is completed. □

Remark 8: From (62), it is clear that $\mathcal{V}$ will not converge to zero for the existence of e_2 owing to estimation error of the ESO. It implies that the state Y_1 can also only converge into a neighborhood of the reference trajectory, and remains within it.

5. SIMULATION RESULTS

This section presents results of simulation for the flight path control of a simplified Navion aircraft model [34], whose flight conditions, aircraft parameters, and derivatives are shown in Table 2.

The complete CLS including the ADRC and ESO is simulated. The initial conditions are $x(0) = y(0) = z(0) = 0$, $\chi(0) = 0$, $\gamma(0) = 0$, $\alpha(0) = \alpha_0 = 0rad$, $\beta(0) = 0$,

Table 2. Flight condition, aircraft parameters, and derivatives.

H	0	m	C_L	0.28	C_{l_β}	-0.26
ρ	1.225	kg/m^3	C_D	0.015	C_{l_p}	-0.36
V	53.5	m/s	C_T	0.015	C_{l_r}	0.10
S_r	17.1	m^2	C_{m_u}	0.017	$C_{l_{\delta a}}$	0.013
l_1	10.15	m	C_{m_α}	-0.60	$C_{l_{\delta r}}$	0.0007
l_2	2.14	m	$C_{m_{\dot\alpha}}$	-2.00	C_{n_β}	0.11
l_3	1.74	m	C_{m_q}	-15.5	C_{n_p}	-0.032
I_x	1420.5	kg·m^2	C_{L_u}	0.43	C_{n_r}	-0.23
I_y	4066.4	kg·m^2	$C_{L\alpha}$	3.4	$C_{n_{\delta a}}$	0.0018
I_z	4784.7	kg·m^2	$C_{L_{\dot\alpha}}$	6	$C_{n_{\delta r}}$	-0.1
I_{xz}	0	kg·m^2	C_{L_q}	5.4	$C_{y_{l\beta}}$	-0.90
V_0	53.5	m/s	C_{D_α}	0.20	C_{y_p}	0
T_x	189.8	N	C_{D_u}	0.0	C_{y_r}	0
m	1247	kg	$C_{L_{\delta e}}$	0.34	$C_{y_{\delta a}}$	0
Pr	0.2695	–	$C_{D_{\delta e}}$	0.0	$C_{y_{\delta r}}$	0.18
M_a	0.158	–	$C_{m_{\delta e}}$	-1.4		

Note: $\frac{\partial C_x}{\partial y} \triangleq C_{x_y}$.

Table 3. Parameters of simulation.

ADRC	σ=0.15	λ_1=120	λ_2=3600	δ=0.1
	κ_1=12	$\kappa_2 = 6$	$\Pi = 3.4I_3$	K_p=100
PID	$k_p = 3$	$k_i = 0.1$	$k_d = 0.01$	–

Note: I_3 represents the $R^{3\times3}$ identity matrix.

$\mu(0) = 0,\ p(0) = q(0) = r(0) = 0,\ \begin{bmatrix} \delta_a & \delta_r & \delta_e \end{bmatrix}^T = \begin{bmatrix} 0.1 & -0.6 & 0 \end{bmatrix}^T (degree)$,

Through the above analysis and proof, it is very important to select properly the gain parameters Π, λ_1 and λ_2. The optimum parameters of the controllers and ESO are selected and obtained in Table 3 by analysis and calculation.

Remark 9: Through proof and analysis, we know the value range of each observation gain, and know which parameters are the bigger the better, and which parameters are the smaller the better. This provides us with a good direction and great convenience for selecting parameter values in simulation experiments. In the simulation experiment, the data in Table 3 was obtained by adjusting the parameters appropriately.

Fig. 3 is the structure diagram of the closed-loop system control strategy, including the control strategy of ADRC and PID.

In practice, both the deflection angle and the deflection rate of the rudder are limited, so the constraint of control input must be considered, and the saturation limiting function sat$(\cdot)$ (As shown in the Fig. 4), the actual control input

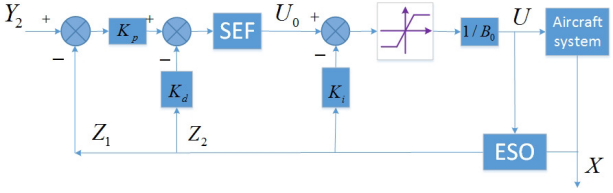

Fig. 3. Block diagram of the closed-loop control.

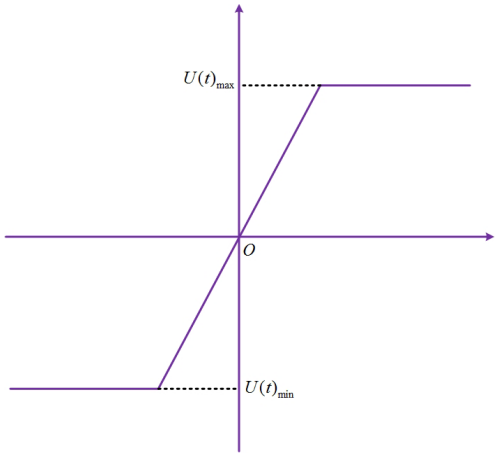

Fig. 4. Schematic diagram of saturation constraint function.

$U(t)$ is expressed as

$$U(t) = \Omega \text{sat}\left(\frac{U_0}{\Omega}\right) = \begin{cases} U(t)_{max}, & U_0 > U(t)_{max}, \\ U_0, & U_0 \in [U(t)_{min}, U(t)_{max}], \\ U(t)_{min}, & U_0 < U(t)_{min}, \end{cases} \tag{63}$$

where Ω is the control domain, and its value range is $[U(t)_{min}, U(t)_{max}]$, $U(t)_{Max}$ is the maximum control quantity allowed to be input, corresponding to the minimum turning radius and the shortest time of adjusting direction.

One reference output trajectory is as follows:

$$Y_r = \begin{bmatrix} \psi_r \\ \theta_r \\ \phi_r \end{bmatrix} = \begin{bmatrix} 2(\text{degree}) \\ -3(\text{degree}) \\ 4(\text{degree}) \end{bmatrix},$$

where the initial attitude angles are

$$\begin{bmatrix} \psi(0) \\ \theta(0) \\ \phi(0) \end{bmatrix} = \begin{bmatrix} 0(\text{degree}) \\ 0(\text{degree}) \\ 0(\text{degree}) \end{bmatrix}.$$

Fig. 5 shows the attitude trajectories. Obviously, by choosing a reasonable parameter Π and K_p, the designed aircraft control system can ensure that the obtained attitude angle can effectively track the controlled angle. In

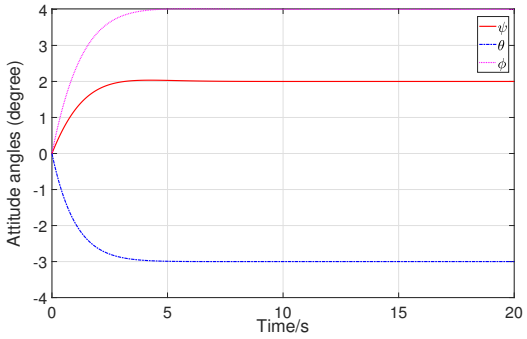

Fig. 5. Attitude angles (degree).

fact, the attitude angle needs less than $4s$ to astringe to the reference states, which meets the system attribute requirement of $T \leq 4s$, where T denotes the time when the system reaches the stable state. In order to quickly obtain the signal $\dot{Y}_r$, the parameters κ_1, κ_2 utilized in TD are chosen as $\kappa_1 = 12, \kappa_2 = 6$.

Figs. 6-8 shows the performances of ESO observing the uncertainties $H(t)$. By choosing proper values of λ_1, λ_2, σ and δ, each component of the estimated states $Z_{2^i}(t)$ astringes to the practical uncertainty component $H_i(t)$ within finite time. Concretely speaking, the estimated states $Z_{2^1}(t)$, $Z_{2^2}(t)$ and $Z_{2^3}(t)$ astringe to the practical uncertainty components $H_1(t)$, $H_2(t)$ and $H_3(t)$ within $0.1s$, $0.3s$ and $0.3s$, respectively. Hence, the application of ESO is reasonable.

Fig. 9 depicts the trajectories of angular velocity. The angular velocity state trajectory converges very fast, and the convergence time is less than 4s. The control input deflections and the derivatives of deflections are shown in Fig. 10 and Fig. 11. The state trajectories are basically stable within 4 seconds and remains there. In order to verify the robust stability of ADRC, we added the external interference in the experimental simulation, which is the Gaussian white noise interference, and the Gaussian white noise Fig. 12 runs through the whole experiment, which is the comparative analysis under the interference of Gaussian white noise. Attack angle, sideslip angle and the homologous derivatives are shown in Figs. 13 and 14. And Fig. 15, Fig. 16, Fig. 17, Fig. 18 under the different controller of PID and SMC, respectively.

Compared with the PID and SMC, the several advantages of our method are obtained as follows:

- Considering the astringency speed of state trajectory, it is obvious that our method converges faster than PID and SMC.
- For ADRC, its overshoot must be considered. The simulation results show that, compared with PID and SMC, the ADRC method proposed in this paper has better robustness and stability.
- From Figs. 13-18 we can discover the state trajectories applied ADRC are smoother than the results applied PID and SMC. This point deserves mentioning for in the process of practical application, the systems may be damaged if the astringency is poor.

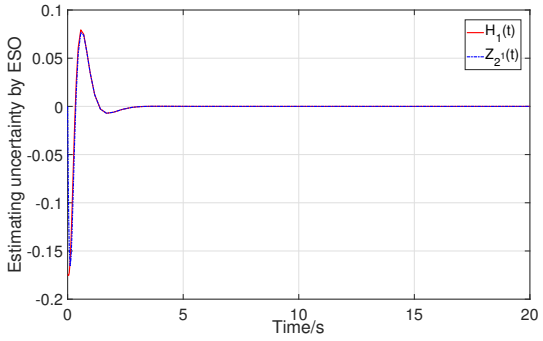

Fig. 6. Estimating uncertainty by ESO.

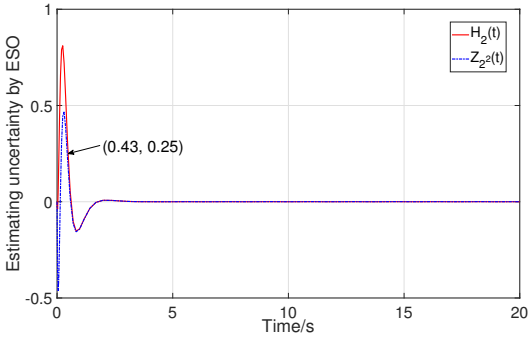

Fig. 7. Estimating uncertainty by ESO.

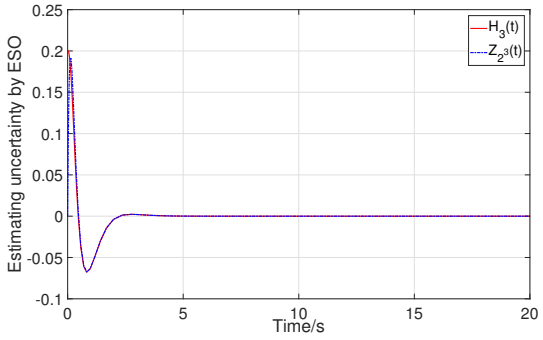

Fig. 8. Estimating uncertainty by ESO.

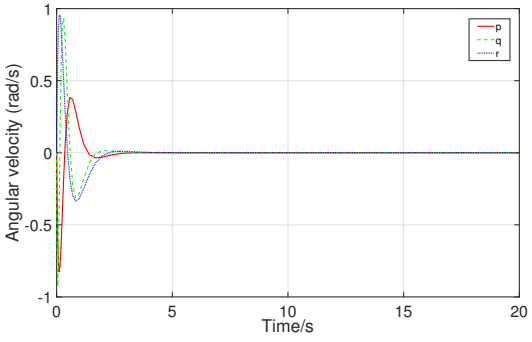

Fig. 9. Angular velocity (rad/s).

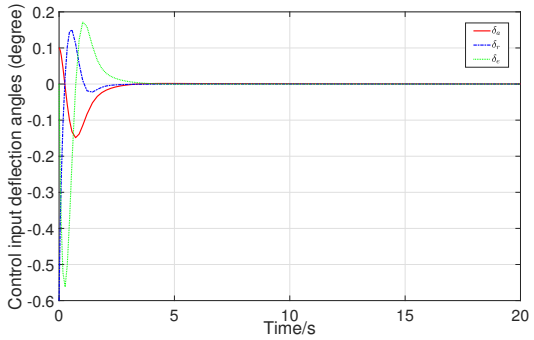

Fig. 10. Control input deflection angles (degree).

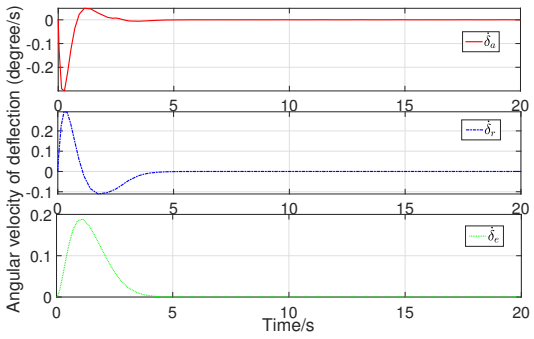

Fig. 11. Angular velocity of deflection (degree/s).

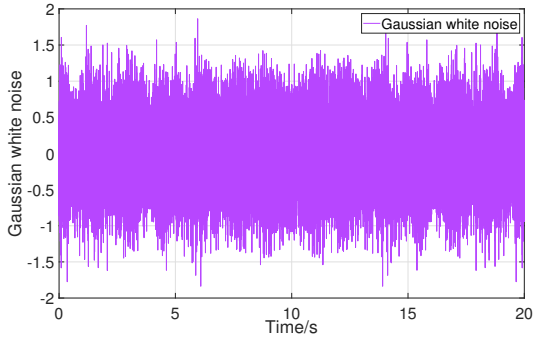

Fig. 12. Gaussian white noise interference.

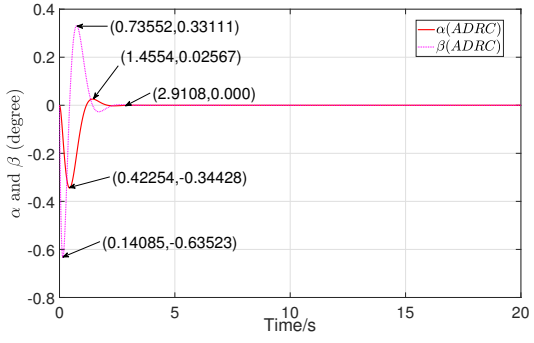

Fig. 13. α and β (degree)(ADRC).

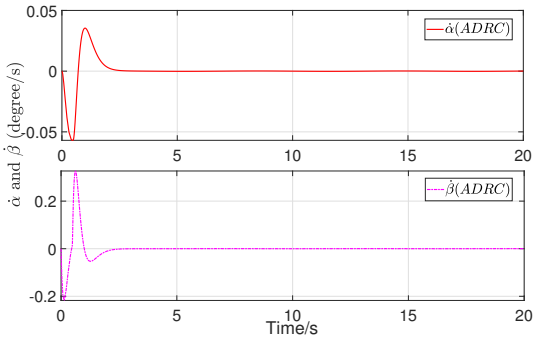

Fig. 14. $\dot{\alpha}$ and $\dot{\beta}$ (degree/s)(ADRC).

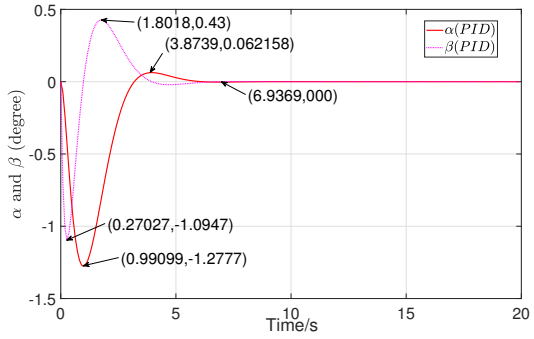

Fig. 15. α and β (degree)(PID).

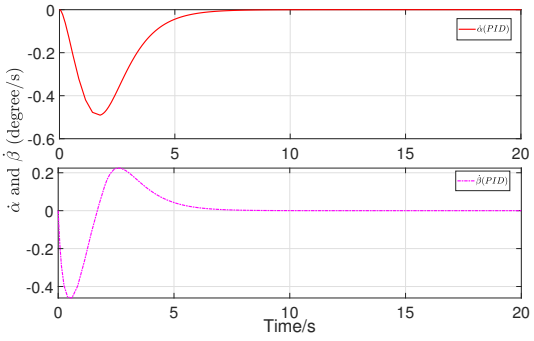

Fig. 16. $\dot{\alpha}$ and $\dot{\beta}$ (degree/s)(PID).

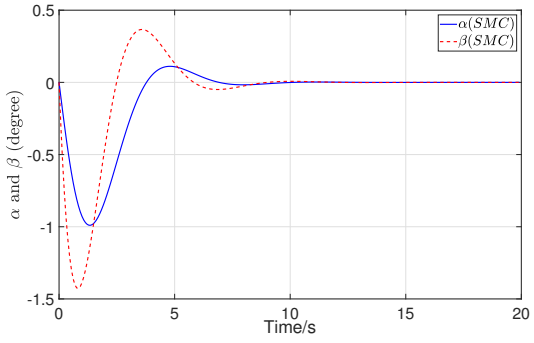

Fig. 17. α and β (degree)(SMC).

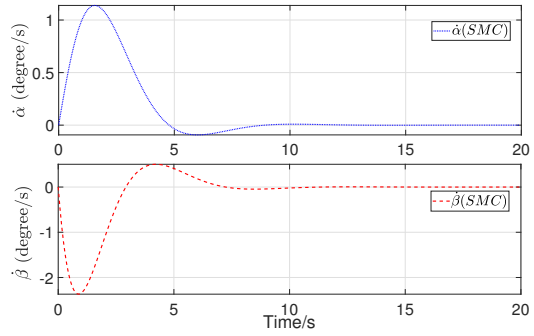

Fig. 18. $\dot{\alpha}$ and $\dot{\beta}$ (degree/s)(SMC).

6. CONCLUSION

This paper has researched the combining the back-stepping and ADRC to research the problem of attitude control for an aircraft model which is non-linear in aerodynamics. Firstly, aircraft model is introduced. Then ESO is applied to estimate the unknown variable $H(t)$ which is considered as external disturbances and the internal dynamics Y_3 and Y_4. Next, ADRC strategy is applied to control attitude control for an aircraft model in comparison with the PID and SMC control approach. The stability of ESO and ADRC are analyzed and proven theoretically. The effectiveness of this method is illustrated with example of Navion aircraft model. The results acquired from simulation attest that the ADRC is able to attain better control performance than the PID and SMC method. The future work should improve the control accuracy and sensitivity of attitude control. Although the control time can be within two seconds, there are obviously some small overshoots, which need further improvement. The flight path tracking and velocity tracking of the powered aircraft will be studied in future. Further study on the performance of non-steady aircraft, including glide at constant angle of attack, glide at constant altitude and so on.

DISCLOSURE STATEMENT

No potential conflict of interest was reported by the authors. No conflict of interest exits in the submission of this manuscript, and manuscript is approved by all authors for publication.

REFERENCES

[1] M. A. Lieberman, A. J. Lichtenberg, and M. V. Cook, *Flight Dynamics Principles: A Linear Systems Approach to Aircraft Stability and Control*, Waltham, USA, 2014.

[2] W. C. Luo, Y. C. Chu, and K. V. Ling, "Inverse optimal adaptive control for attitude tracking of spacecraft," *IEEE Transactions on Automatic Control*, vol. 50, no. 11, pp. 1639-1654, December 2005.

[3] X. H. Nian, W. Q Chen, X. Y. Chu, and Z. W. Xu, "Robust adaptive fault estimation and fault tolerant control for quadrotor attitude systems," *International Journal of Control*, vol. 93, no. 3, pp. 725-737, 2020.

[4] H. Lee and Y. Kim, "Fault-tolerant control scheme for satellite attitude control system," *IET Control Theory & Applications*, vol. 4, no. 8, pp. 1436-1450, 2010.

[5] X. Liang, Q. Wang, C. Hu, and C. Dong, "Observer-based H_∞ fault-tolerant attitude control for satellite with actuator and sensor faults," *Aerospace Science and Technology*, vol. 95, pp. 105424, September 2019.

[6] Z. J. Zhou, X. S. Wang, and Y. Wang, "Spacecraft attitude control based on fuzzy adaptive algorithm," *Electric Machines and Control*, vol. 23, no. 2, pp. 123-128, February 2019.

[7] Y. Wang, M. Chen, Q. Wu, and J. Zhang, "Fuzzy adaptive non-affine attitude tracking control for a generic hypersonic flight vehicle," *Aerospace Science and Technology*, vol. 80, pp. 56-66, July 2018.

[8] L. G. Gong, Q. Wang, and C. Y. Dong, "Switching disturbance rejection attitude control of near space vehicles with variable structure," *Journal of Systems Engineering and Electronics*, vol. 30, no. 1, pp. 167-179, 2019.

[9] T. Cao, H. J. Gong, and B. Han, "Sliding mode fault tolerant attitude control scheme for spacecraft with actuator faults," *Transactions of Nanjing University of Aeronautics and Astronautics*, vol. 36, no. 01, pp. 123-131, 2019.

[10] W. Gong, B. Li, Y. Yang, H. Ban, and B. Xiao, "Fixed-time integral-type sliding mode control for the quadrotor UAV attitude stabilization under actuator failures," *Aerospace Science and Technology*, vol. 95. pp. 105444, 2019.

[11] X. Shao and H. Wang, "Active disturbance rejection based trajectory linearization control for hypersonic reentry vehicle with bounded uncertainties," *ISA Transactions*, vol. 54, pp. 27-38, 2015.

[12] L. Wang and J. Su, "Trajectory tracking of vertical take-off and landing unmanned aerial vehicles based on disturbance rejection control," *IEEE/CAA Journal of Automatica sinica*, vol. 2, no. 1, pp. 65-73, 2015.

[13] M. R. Mokhtari, B. Cherki, and A. C. Braham, "Disturbance observer based hierarchical control of coaxial-rotor UAV," *ISA Transactions*, vol. 67, pp. 466-475, 2017.

[14] M. R. Mokhtari, A. C. Braham, and B. Cherki, "Extended observer based control for a coaxial-rotor UAV," *ISA Transactions*, vol. 61, no. 1, pp. 1-14, 2016.

[15] H. A. Ronald, "Analysis of aircraft attitude control systems prone to pilot-induced oscillations," *Journal of Guidance Control & Dynamics*, vol. 7, no. 1, 106-112, 1984.

[16] C. Y. Fu, W. Hong, H. Q. Lu, L. Zhang, X. J. Guo, and Y. T. Tian, "Adaptive robust backstepping attitude control for a multi-rotor unmanned aerial vehicle with time-varying output constraints," *Aerospace Science and Technology*, vol. 78, pp. 593-603, May 2018.

[17] M. Zarei, M. Arvan, A. Vali, and F. Behazin, "Backstepping sliding mode control of one degree of freedom flight motion table," *Asian Journal of Control*, vol. 22, no. 4, pp. 1700-1713, July 2020.

[18] C. Zhang, Z. J. Chen, and C. Wei, "Sliding mode disturbance observer-based backstepping control for a transport aircraft," *Science China*, no. 05, pp. 228-243, 2014.

[19] J. Han, "Auto-disturbances-rejection controller and its applications," *Control & Decision*, vol. 13, no. 1, pp. 19-23, 1998.

[20] Z. Gao, Y. Huang, and J. Han, "An alternative paradigm for control system design," *Proc. of the 40th IEEE Conference on Decision and Control*, 2001. DOI: 10.1109/CDC.2001.980926

[21] Z. Gao, "Scaling and parameterization based controller tuning," *Proc. of the American Control Conference*, pp. 4989-4996, 2003.

[22] J. Han, "The extended state observer of a class of uncertain systems," *Control & Decision*, vol. 10, no. 1, pp. 85-88, 1995.

[23] Q. Zheng, L. Q. Gao, and Z. Gao, "On validation of extended state observer through analysis and experimentation," *Journal of Dynamic Systems Measurement & Control*, vol. 134, no. 2, pp. 024505(1-6), 2012.

[24] J. Han, "From PID to active disturbance rejection control," *IEEE Transactions on Industrial Electronics*, vol. 56, no. 3, pp. 900-906, 2009.

[25] B. Z. Guo and Z. L. Zhao, *Active Disturbance Rejection Control for Nonlinear Systems: An Introduction*, John Wiley & Sons, Singapore Pte. Ltd., 2016.

[26] Z. Q. Chen, M. W. Sun, and R. G. Yang, "On the stability of linear active disturbance rejection control," *Acta Automatica Sinica*, vol. 39, no. 5, pp. 574-580, 2013.

[27] S. N. Singh, M. L. Steinberg, and A. B. Page, "Nonlinear adaptive and sliding mode flight path control of F/A-18 model," *IEEE Transactions on Aerospace & Electronic Systems*, vol. 39, no. 4, pp. 1250-1262, 2003.

[28] A. Miele and R. E. Street, "Flight mechanics theory of flight paths," *Physics Today*, vol. 16, no. 1, pp. 66-68, 2016.

[29] Y. Q. Xia, P. Shi, G. P. Liu, D. Rees, and J. Q. Han, "Active disturbance rejection control for uncertain multivariable systems with time-delay," *IET Control Theory & Applications*, vol. 1, no. 1, pp. 75-81, 2007.

[30] Y. Xia, Z. Zhu, and M. Fu, "Back-stepping sliding mode control for missile systems based on an extended state observer," *IET Control Theory & Applications*, vol. 5, no. 1, pp. 93-102, 2011.

[31] H. Khalil, *Nonlinear Systems*, 1st ed., vol. 10, Springer-Verlag, New York, USA, 2007.

[32] Y. Huang, "A new synthesis method for uncertain systems the self-stable region approach," *International Journal of Systems Science*, vol. 30, no. 1, pp. 33-38, 1999.

[33] Q. Zheng, L. Dong, D. H. Lee, and Z. Gao, "Active disturbance rejection control for mems gyroscopes," *IEEE Transactions on Control Systems Technology*, vol. 17, no. 6, pp. 1432-1438, 2008.

[34] D. K. Schmidt, *Modern Flight Dynamic*, 1st ed., McGraw-Hill Higher Education, 2012.

[35] Z. Yan, H. Yu, W. Zhang, B. Li, and J. Zhou, "Globally finite-time stable tracking control of underactuated UUVs," *Ocean Engineering*, vol. 107, no. 1, pp. 132-146, 2015.

[36] S. P. Bhat and D. S. Bernstein, "Finite-time stability of continuous autonomous systems," *SIAM Journal on Control and Optimization*, vol. 38, no. 3, pp. 751-766, 2000.

[37] S. Yu, X. Yu, B. Shirinzadeh, and Z. Man, "Continuous finite-time control for robotic manipulators with terminal sliding mode," *Automatica*, vol. 41, no. 11, pp. 1957-1964, 2005.

[38] X. Huang, W. Lin, and B. Yang, "Global finite-time stabilization of a class of uncertain nonlinear systems," *Automatica*, vol. 41, no. 5, pp. 881-888, 2005.

[39] S. Li and Y. Tian, "Finite-time stability of cascaded time-varying systems," *International Journal of Control*, vol. 80, no. 4, pp. 646-657, 2007.

Huixuan Zhuang received his B.S. degree in mathematics and applied mathematics from Shenyang University of Technology, Shenyang, China, in 2014 and received an M.S. degree in systems theory from Northeastren University, Shenyang, China, in 2017, and he is currently working toward a Ph.D. degree in control science and engineering at Nankai University, Tianjin, China. His research interests include sliding mode control, disturbance rejection control, and system modeling.

Qinglin Sun received his B.E. and M.E. degrees in control theory and control engineering from Tianjin University, Tianjin, China, in 1985 and 1990, respectively, and a Ph.D. degree in control science and engineering from Nankai University, Tianjin, China, in 2003. He is currently a Professor in the Intelligence Predictive Adaptive Control Laboratory and the College of Artificial Intelligence, Nankai University. He has published more than 100 peer-reviewed papers. His research interests include self-adaptive control, modeling and control of flexible spacecraft, complex systems, and embedded control systems and their applications.

Zengqiang Chen received his B.S. degree in mathematics and his M.S. and Ph.D. degrees in automatic control from Nankai University, Tianjin, China, in 1987, 1990, and 1997, respectively. He is currently a Full Professor in the Department of Automation, College of Artificial Intelligence, Nankai University. He has authored or coauthored more than 200 journal papers. His current research interests include intelligent optimizing control, intelligent computing, complex networks, andmulti-agent systems.

Xianyi Zeng received his B.Eng. degree from Tsinghua University, Beijing, China, in 1986, and a Ph.D. degree from the Centre d'Automatique, Université des Sciences et Technologies de Lille, Villeneuve-d'Ascq, France, in 1992. He is currently a Professor with the Ecole Nationale Supérieure des Arts et Industries Textiles, Roubaix, France. His research interests include intelligent decision support systems for fashion and material design and modeling and analysis of human perception and cognition on industrial products and their integration into virtual products.